Available online at www.sciencedirect.com

SciVerse ScienceDirect

Ceramics International 38 (2012) 4495–4500

CERAMICS INTERNATIONAL

www.elsevier.com/locate/ceramint

Morphology-controlled synthesis of tungsten oxide hydrates crystallites via a facile, additive-free hydrothermal process

Li Jiayin [a,b], Huang Jianfeng [a,*], Wu Jianpeng [a], Cao Liyun [a], Kazumichi Yanagisawa [b]

[a] *Key Laboratory of Auxiliary Chemistry & Technology for Light Chemical Industry, Ministry of Education, Shaanxi University of Science and Technology, Xi'an 710021, PR China*

[b] *Research Laboratory of Hydrothermal Chemistry, Faculty of Science, Kochi University, 2-5-1 Akebono-cho, Kochi 780-8520, Japan*

Received 22 November 2011; received in revised form 31 January 2012; accepted 8 February 2012
Available online 17 February 2012

Abstract

Tungsten oxide hydrates crystallites with a diversity of morphologies were successfully synthesized by employing peroxo-polytungstic acid as the precursor via a facile and additive-free hydrothermal process. The crystal structure, morphology and orientation relationship were investigated by using X-ray diffractometer, scanning electron microscopy and transmission electron microscopy. Results show that with the increase of the hydrothermal reaction time, the product morphology shows an obvious evolution from hexagonal plates to round angular blocks and to hexagonal gears, through irregular nanosheets and to cuboid rods finally. Furthermore, the driving force of this morphology evolution was found to be correspondent with the interesting change of the orientation growth and the phase transition of tungsten oxide hydrates under the hydrothermal process.

Keywords: A. Grain growth; D. Transition metal oxides; Morphology evolution; Hydrothermal process

1. Introduction

The past decade has witnessed a rapid development of the activities in the synthesis of new nanoparticles, driven both by the intense interest of exploring new science and by the hope for the potential applications and economic impacts [1,2]. At present, one of the largest activities in this field has been focused on the size and morphology design and controlling of the metal oxide particles in order to achieve fascinating properties in technological applications. Thus, an increasing number of works have been reported to successfully synthesize these materials with desired morphologies using solution-based method, such as ZnO [3], CuO [4], TiO_2 [5], Fe_2O_3 [6], CeO_2 [7], and WO_3 [8]. Nevertheless, as difficulties in practicability and economical proficiency remain, it is still of great significance to develop the synthesis of nanostructured materials with shape-dependent properties, which will result in a wide range of electrical, optical, catalytic, or thermal properties and inspire new domains of theoretical research and better their technological applications.

As one kind of well-known functional metal oxides, tungsten oxide and its hydrates ($WO_3{\cdot}nH_2O$, $n = 0$–2) have been extensively researched and employed in various fields including supercapacitors [9], photo catalysts [10,11], gas sensors [10,11], chromic devices [10,11], and water treatment [10,11]. These applications highlight the profound significance of the morphology control to exhibit the strong connections between the product morphology and properties [12]. However, contaminations are usually created during production and economic efficiency loss is unavoidable in practical applications, for organic [13] or inorganic [14] templates are often necessary to achieve the specific morphologies. Thus, the synthesis of $WO_3{\cdot}nH_2O$ particles by template-free methods have made great achievements [14–16] but still have limitations in controlling specific morphologies, which involves extremely poisonous starting materials [17,18], or expensive tungsten sources like $W(CO)_6$ [19] and $W(Cl)_6$ [14,15,20–23]. As a tungsten-base water-soluble precursor, peroxo-polytungstic acid can be obtained by simply mixing tungsten powders with hydrogen peroxide solution. This acid has been reported to

* Corresponding author. Tel.: +86 29 86168803; fax: +86 29 86168803.
E-mail addresses: huangif@163.com, smlglw@foxmail.com (H. Jianfeng).

0272-8842/$36.00 © 2012 Published by Elsevier Ltd and Techna Group S.r.l.
doi:10.1016/j.ceramint.2012.02.025

synthesize sheets-like $WO_3{\cdot}nH_2O$ particles before [14], but few works of controlling different morphology using this acid have been reported yet. Therefore, the synthesis of $WO_3{\cdot}nH_2O$ particles using peroxo-tungstic acid by solution-based method, especially without any additives, are expected to widely enhance the practical applications of tungsten oxide hydrates materials. In the present work, a facile, additive-free synthesis of $WO_3{\cdot}nH_2O$ particles with controlled morphology evolution and phase transition under hydrothermal conditions is reported. Peroxo-polytungstic acid was used in this method as the precursor to achieve three-dimensional morphology evolution for the first time. A possible growth mechanism of the morphology evolution was suggested to reveal the growth habits of $WO_3{\cdot}nH_2O$ particles when peroxo-polytungstic acid is used as the precursor in hydrothermal reactions.

2. Experimental

2.1. Preparation of peroxo-polytungstic acid solution

The $WO_3{\cdot}0.33H_2O$ particles were synthesized by a hydrothermal reaction using peroxo-polytungstic acid as precursor solutions. In a typical synthesis process, finely powdered tungsten (4 g, wako, 12 μm) was slowly added to hydrogen peroxide (20 mL, 30 wt%, wako) in a cold water bath (10 °C) to stabilize the reaction temperature below 40 °C. This produced a clear and colorless peroxo-polytungstic acid solution.

2.2. Synthesis of tungsten oxide hydrates particles

The as-prepared solution was then diluted in deionized water to obtain a tungsten concentration of 0.127 mol/L. After that, the diluted solution was transferred into a Teflon-lined stainless steel autoclave (25 mL, filling ratio 60%), and the autoclave was then sealed and maintained at 180 °C for 1 h. After cooled to room temperature, the as-prepared precipitates were isolated by centrifugation and repeatedly washed with absolute ethanol (5 mL) for four times. Finally, the as-obtained precipitates were dried at 40 °C in a drying cabinet for 1 h. To explore the morphology evolution, the reaction times varied from 1 h to 96 h while other conditions were kept unchanged.

2.3. Characterization

The phase composition of the samples was characterized via X-ray powder diffraction (XRD) on a Ultima IV X-ray diffractometer with Cu Kα radiation ($\lambda = 0.15406$ nm) at a scanning rate of 8° min^{-1} (Rigaku, Japan) in the 2θ range from 10° to 70°. A JSM-6500F field-emission scanning electron microscope was used for the observation of field emission scanning electron microscopic (FESEM) images. Transmission electron microscopic (TEM) images, high-resolution transmission electron microscopic (HRTEM) images and selected area electron diffractions (SAED) were taken on a JEM-3010 high-resolution transmission electron microscope operated at 300 kV.

3. Results and discussion

3.1. The phase transition

The XRD patterns of the products prepared at different hydrothermal reaction time are shown in Fig. 1. The sample prepared at first 4 h give rise to similar XRD pattern that can be indexed to orthorhombic $WO_3{\cdot}0.33H_2O$ phase (JCPDS Card No. 87-1203). When the reaction time reaches to 24 h, three XRD peaks of monoclinic WO_3 (JCPDS Card No. 71-2141) are observed, revealing the existence of a phase transition from orthorhombic $WO_3{\cdot}0.33H_2O$ to monoclinic WO_3. This transition are further demonstrated with hydrothermal reaction time increased to 96 h, at which the strong peak intensity XRD peaks of monoclinic WO_3 with weak peak intensity of orthorhombic $WO_3{\cdot}0.33H_2O$ are found.

3.2. The morphology evolution

By using the peroxo-polytungstic acid as the precursor, we aim to take advantage of the chelating peroxo ligands to achieve three-dimensional microstructure with potential different functional properties. In the course of our research, it is shown that this precursor can lead to obvious different morphologies compared with other previous reports [14]. With the reaction time increased, the SEM images of the crystallites are shown in Fig. 2, which exhibit obvious morphology evolution, from flat hexagonal $WO_3{\cdot}0.33H_2O$ plates (Fig. 2a) to round angular blocks (Fig. 2b) and to hexagonal gears (Fig. 2c), through irregular nanosheets (Fig. 2d), and to, ultimately, cuboid WO_3 rods (Fig. 2e). At short reaction time (1 h), the sample appears to be orthorhombic $WO_3{\cdot}0.33H_2O$ with flat hexagonal plate-like morphology with branch-like structure inside (Fig. 2a). It is found that every hexagonal plate-like structure has sheets-like structures in six symmetric oriented growth directions parallel to the plane of the plates. When the reaction time is controlled at 2 h (Fig. 2b), the hexagonal plates become thicker and are more like spheres with hexagonal edges and corners. This indicates that the crystal growth direction may switch to a

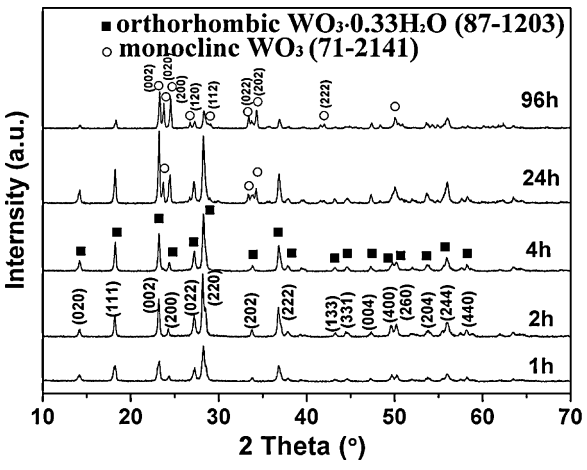

Fig. 1. XRD patterns of the products prepared by using peroxo-polytungstic acid with different hydrothermal reaction times.

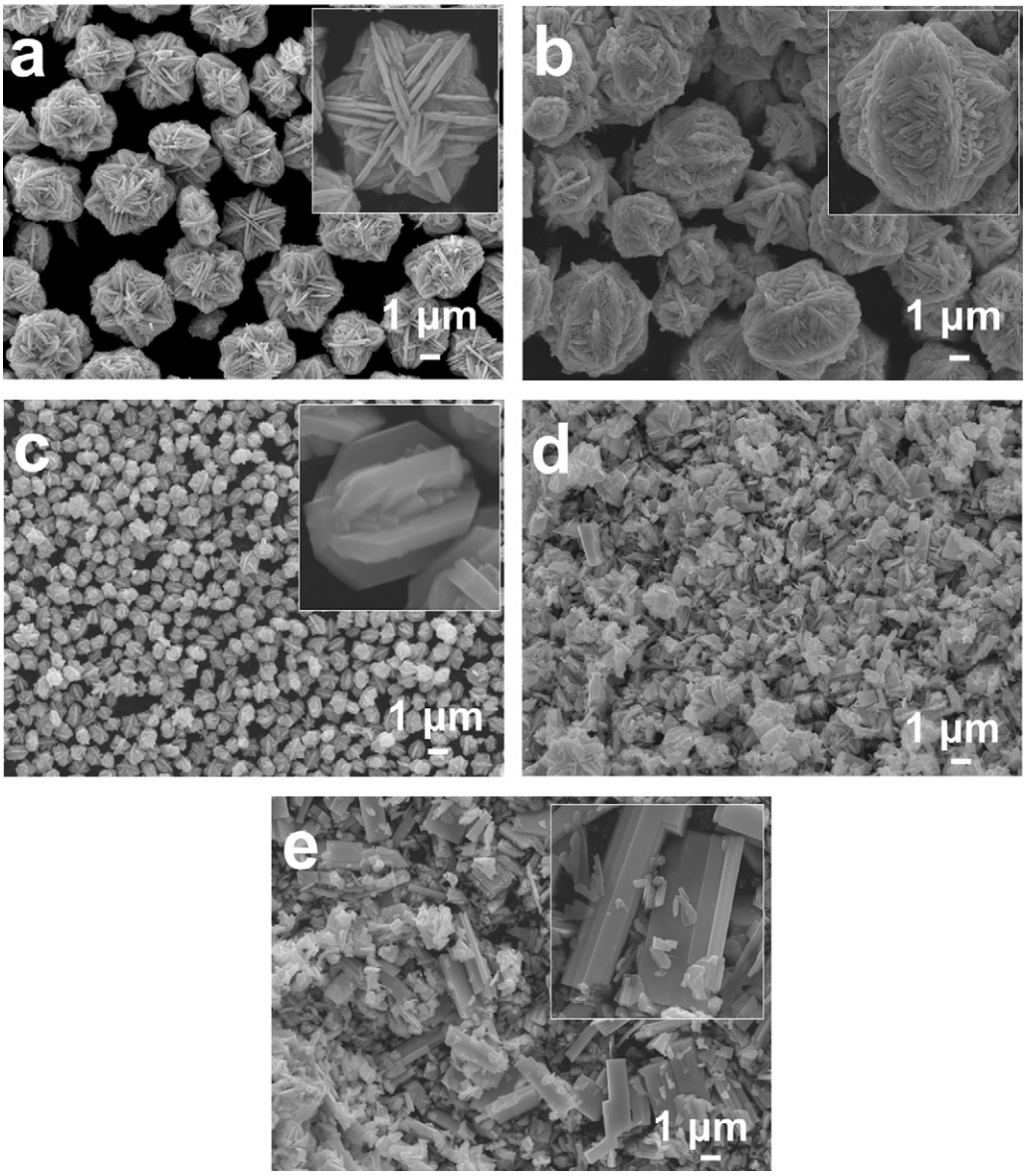

Fig. 2. SEM images of the products prepared by using peroxo-polytungstic acid as precursor under different hydrothermal reaction times: (a) 1 h; (b) 2 h; (c) 4 h; (d) 24 h; (e) 96 h.

direction that is perpendicular to the plates to form the hierarchical three-dimensional structures. This perpendicular growth is further maintained to 4 h (Fig. 2c), where hexagonal gears-like particle with much smaller size (∼1 μm) is found. Further observation of the particles in the inset in Fig. 2c reveals that smooth surfaces and clear edges and corners are formed, implying that these particles may be well crystallized through the ''Oswald ripening'' process in which the particles tend to have uniform size and more regular shapes rather than hierarchical structures. When reaction time arrives at 24 h, irregular sheets are obtained, showing that the irregular shapes may result from the breaking of the former structures. Furthermore, cuboid rods are found when the reaction time is prolonged to 96 h (Fig. 2e), indicating the existence of a recrystallization process after the breaking of the former structures. Referring to the XRD pattern in Fig. 1 (24 h), it is suggested that the breaking of the former structures may be attributed to the phase transition from orthorhombic $WO_3{\cdot}0.33H_2O$ to monoclinic WO_3. This monoclinic WO_3 phase may be further considered as the cuboid WO_3 rods found in Fig. 2e, being in accordance well with the phase transition discussed in the XRD results.

3.3. The change of orientation growth

TEM images (Fig. 3) were taken for detailed information of the crystallites growth during the morphology evolution. Fig. 3a is a typical TEM image of a hexagonal plate-like particle with reaction time of 1 h, showing similar morphology as observed in the SEM image (inserted in Fig. 3a). Further observation reveals that the plate is composed of many sheets-like structures regularly arranged in six directions. The six directions are confirmed by the corresponding selected area electron diffraction pattern (SAED) inserted in Fig. 3a. This pattern

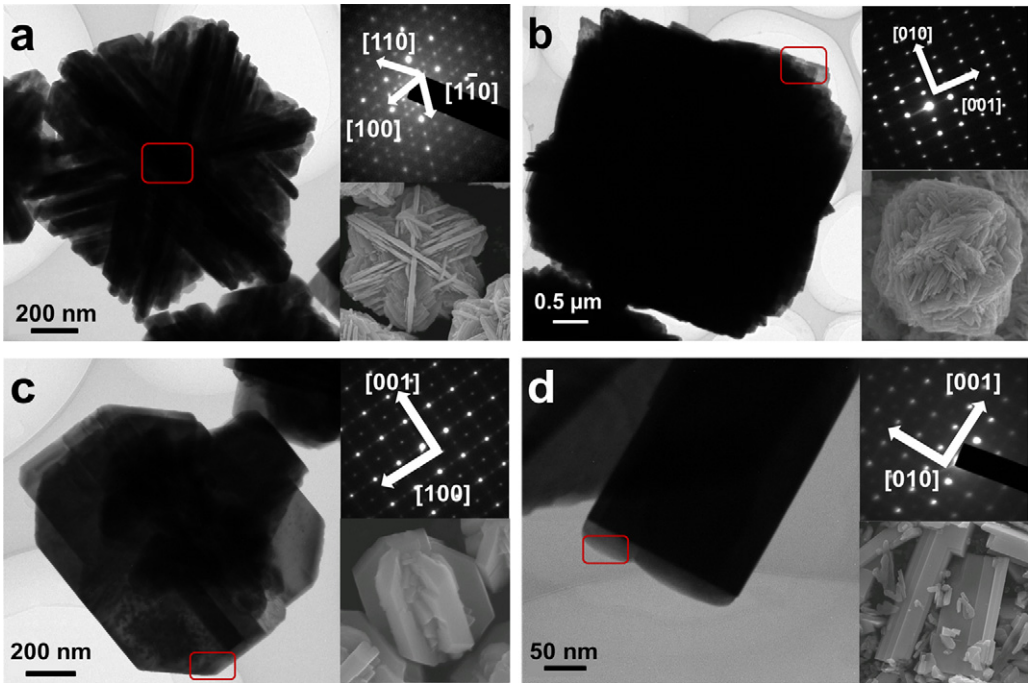

Fig. 3. TEM (left) images of the products prepared with different reaction times: (a) 1 h; (b) 2 h; (c) 4 h; (d) 96 h. Corresponding SAED patterns and SEM images of similar particles were inserted as upper and lower insets (right) in the TEM images, respectively. The SAED patterns were obtained at the center of the red rectangles in the TEM images. (For interpretation of the references to color in this figure legend, the reader is referred to the web version of the article.)

could be indexed to the [0 0 1] zone axis of orthorhombic $WO_3{\cdot}0.33H_2O$, which indicates that the hexagonal plate-like structure resulted from the oriented crystal growth along six directions that parallel to (0 0 1) plane: ±[1 1 0], ±[1 0 0] and ±[1 $\bar{1}$ 0]. In Fig. 3b, an outline of the round angular blocks is shown in the TEM image, in which the particle has a size of ~4 μm and a similar outline compared to the SEM image inserted in Fig. 3b. The corresponding SAED pattern that was taken from the area marked in red in Fig. 3b shows the [1 0 0] zone axis with diffraction spots along the [0 1 0] and [0 0 1] directions. This reveals that when the reaction time increases to 2 h, the hexagonal plates change their oriented crystal growth directions to [0 0 1] direction to form the three-dimensional round angular block structure. Such change is maintained until the reaction time is extended to 4 h, leading to a hexagonal gears-like structure in Fig. 3c. According to the TEM image and SAED pattern, the hexagonal gears-like structure is suggested to be generated from a three-dimensional growth along [0 0 1] direction that is perpendicular to (0 0 1) plane and other six directions that are parallel to (0 0 1) plane. As for the rod-like particles prepared at 96 h, corresponding TEM image and SAED pattern are shown in Fig. 3d. The SAED pattern in Fig. 3d can be indexed to [1 0 0] zone axis of monoclinic WO_3 with the orientation along [0 0 1] direction, indicating that the rod-like structure is produced from the phase transition from orthorhombic $WO_3{\cdot}0.33H_2O$ to monoclinic WO_3.

3.4. The growth mechanism of the tungsten oxide hydrates

The growth mechanism of all the nano/microstructures of tungsten oxide hydrates during the morphology evolution process can be readily understandable now. The change of their orientation growth and phase transition are believed to be the key factors of the morphology evolution. These changes are shown in a schematic illustration in Fig. 4. Clearly, orthorhombic $WO_3{\cdot}0.33H_2O$ is obtained within the reaction time from 1 h to 4 h. From the beginning (1 h), the particles are found to have hexagonal plate-like shapes with regularly arranged sheets-like structures growing along six directions, ±[1 1 0], ±[1 0 0] and ±[1 $\bar{1}$ 0], which are parallel to the (0 0 1) plane. The formation of this hexagonal plate-like orthorhombic $WO_3{\cdot}0.33H_2O$ particles is similar to the previous works reported by Zhou [15,23]. However, when the reaction time reaches 2 h, the growth orientation will turn to [0 0 1] direction

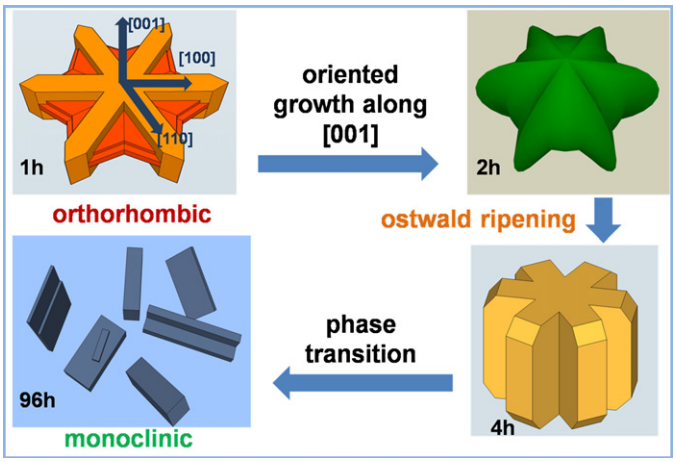

Fig. 4. Schematic illustration of the morphology evolution using peroxo-polytungstic acid as the precursor.

to form round angular block structure with hexagonal corners and edges, which is shown in Fig. 4. Such an interesting change of the growth orientation has not been reported before. This change of the growth orientation may result from the decreased supersaturation of the solute and the polar crystal growth during the hydrothermal reaction process. In the nucleus growth stage, nucleation has occurred at relatively high supersaturation, which is favorable for the formation of $WO_3{\cdot}0.33H_2O$ hexagonal plate-like shapes. As the supersaturation of the solution is decreased to relatively low value after solute is consumed for the nucleus formation, polar crystal growth may predominate to led to the formation of round angular block structure with hexagonal corners and edges, which may be considered as the results of favorable growth along [1 0 0] directions. Thus, a three-dimensional growth along [0 0 1] direction that is perpendicular to (0 0 1) plane and other six directions that are parallel to (0 0 1) plane is found at the reaction time of 2 h. Similar change of growth orientation are found by Li et al. [24] and Chen et al. [25], who successfully explained the growth change of the polar ZnO and dipolar Cu_2O crystals. Both of them reported the changes of growth habits are simultaneously influenced by both supersaturation of the solute and the polar growth habits of their crystals. When the reaction time increases to 4 h, the round angular blocks will further change to gears-like structures with clear hexagonal corners and edges. This is may result from the ''Oswald ripening'' process to obtain more regular shapes of the as-prepared particles. Moreover, the much smaller particle size may be related to the change of the precursor solution, where the protons decrease with increased pH value during the $WO_3{\cdot}nH_2O$ precipitation process [26]. This increased pH value in reaction solution is suggested to effectively influence the grain sizes during the dissolution of the precursor. Similar results have been reported by Wu et al. to reveal the effect of pH value on the sizes of CeO_2 particles grown through ''Ostwald ripening'' process under hydrothermal conditions [27]. As the reaction time is prolonged to 24 h, the phase transition from orthorhombic $WO_3{\cdot}0.33H_2O$ to monoclinic WO_3 with irregular sheets-like structures is observed, indicating that the dissolution of the crystallized structure tends to dominate during the phase transition process. This transition will continue to form the monoclinic WO_3 phase when the reaction time arrives at 96 h. The particles in this phase are finally shaped in rods-like structure with growth orientation along [0 0 1] direction.

4. Conclusion

In summary, the morphology of tungsten oxide hydrates particles has been successfully controlled using peroxo-polytungstic acid as the precursor under hydrothermal conditions. Results exhibit that the particle shapes evolve with reaction times from hexagonal plates to round angular blocks, to three-dimensional hexagonal gears, through irregular sheets to ultimately cuboid rods. As is shown from the growth mechanism, the key factors are believed to be the change of the particle growth orientation and phase transition during the hydrothermal reaction. Our research provides a facile method to maintain different morphologies and phases of tungsten oxide hydrate particles without adding any additives. This approach suggests that peroxo-polytungstic acid may be more applicable in large-scale and green syntheses of other tungsten oxide hydrates that involve well-defined shapes and precisely controlled morphologies.

Acknowledgements

The authors are grateful to Research and National Natural Science Foundation of China (No. 50942047), Natural Science Special Foundation of Shaanxi Education Department (No. 2010JK444), Natural Science Special Projects of Shaanxi Education Department(11JK0820), Innovation Team Assistance Foundation of Shaanxi University of Science and Technology (No. TD09-05), and the Graduate Innovation Fund of Shaanxi University of Science and Technology. The authors are also grateful to Mrs. Yao Chunyan from Shaanxi University of Science and Technology for polishing the paper writing.

References

[1] C. Burda, X. Chen, R. Narayanan, M.A. El-Sayed, Chemistry and properties of nanocrystals of different shapes, Chem. Rev. 105 (2005) 1025–1102.
[2] Y. Zhu, T. Mei, Y. Wang, Y. Qian, Formation and morphology control of nanoparticles via solution routes in an autoclave, J. Mater. Chem. 21 (2011) 11457–11463.
[3] S. Cho, S.-H. Jung, K.-H. Lee, Morphology-controlled growth of ZnO nanostructures using microwave irradiation: from basic to complex structures, J. Phys. Chem. C 112 (2008) 12769–12776.
[4] G.R. Bourret, R.B. Lennox, 1D $Cu(OH)_2$ nanomaterial synthesis templated in water microdroplets, J. Am. Chem. Soc. 132 (2010) 6657–6659.
[5] W. Zhou, X. Liu, J. Cui, D. Liu, J. Li, H. Jiang, J. Wang, H. Liu, Control synthesis of rutile TiO_2 microspheres, nanoflowers, nanotrees and nanobelts via acid-hydrothermal method and their optical properties, CrystEngComm 13 (2011) 4557–4563.
[6] J.-S. Xu, Y.-J. Zhu, [small alpha]-Fe_2O_3 hierarchically hollow microspheres self-assembled with nanosheets: surfactant-free solvothermal synthesis, magnetic and photocatalytic properties, CrystEngComm 13 (2011) 5162–5169.
[7] L. Yan, R. Yu, J. Chen, X. Xing, Template-free hydrothermal synthesis of CeO_2 nano-octahedrons and nanorods: investigation of the morphology evolution, Cryst. Growth Des. 8 (2008) 1474–1477.
[8] J. Wang, P.S. Lee, J. Ma, One-pot synthesis of hierarchically assembled tungsten oxide (hydrates) nano/microstructures by a crystal-seed-assisted hydrothermal process, Cryst. Growth Des. 9 (2009) 2293–2299.
[9] S. Yoon, E. Kang, J.K. Kim, C.W. Lee, J. Lee, Development of high-performance supercapacitor electrodes using novel ordered mesoporous tungsten oxide materials with high electrical conductivity, Chem. Commun. 47 (2011) 1021–1023.
[10] J. Kim, C.W. Lee, W. Choi, Platinized, WO_3 as an environmental photocatalyst that generates OH radicals under visible light, Environ. Sci. Technol. 44 (2010) 6849–6854.
[11] T. Arai, M. Yanagida, Y. Konishi, Y. Iwasaki, H. Sugihara, K. Sayama, Efficient complete oxidation of acetaldehyde into CO_2 over $CuBi_2O_4$/WO_3 composite photocatalyst under visible and UV light irradiation, J. Phys. Chem. C 111 (2007) 7574–7577.
[12] X.-L. Li, T.-J. Lou, X.-M. Sun, Y.-D. Li, Highly sensitive WO_3 hollow-sphere gas sensors, Inorg. Chem. 43 (2004) 5442–5449.
[13] S. Balaji, Y. Djaoued, A.-S. Albert, R. Bruning, N. Beaudoin, J. Robichaud, Porous orthorhombic tungsten oxide thin films: synthesis, characterization,

and application in electrochromic and photochromic devices, J. Mater. Chem. 21 (2011) 3940–3948.
[14] S. Jeon, K. Yong, Morphology-controlled synthesis of highly adsorptive tungsten oxide nanostructures and their application to water treatment, J. Mater. Chem. 20 (2010) 10146–10151.
[15] W. Hu, Y. Zhao, Z. Liu, C.W. Dunnill, D.H. Gregory, Y. Zhu, Nanostructural evolution from one-dimensional tungsten oxide nanowires to three-dimensional ferberite flowers, Chem. Mater. 20 (2008) 5657–5665.
[16] J. Yu, L. Qi, Template-free fabrication of hierarchically flower-like tungsten trioxide assemblies with enhanced visible-light-driven photocatalytic activity, J. Hazard. Mater. 169 (2009) 221–227.
[17] A. Yella, M.N. Tahir, S. Meuer, R. Zentel, R.d. Berger, M. Panthofer, W. Tremel, Synthesis, characterization and hierarchical organization of tungsten oxide nanorods: spreading driven by Marangoni flow, J. Am. Chem. Soc. 131 (2009) 17566–17575.
[18] Z. Wang, S. Zhou, L. Wu, Preparation of rectangular $WO_3{\cdot}H_2O$ nanotubes under mild conditions, Adv. Funct. Mater. 17 (2007) 1790–1794.
[19] E. Kang, S. An, S. Yoon, J.K. Kim, J. Lee, Ordered mesoporous WO_{3-X} possessing electronically conductive framework comparable to carbon framework toward long-term stable cathode supports for fuel cells, J. Mater. Chem. 20 (2010) 7416–7421.
[20] J. Zhang, J.-p. Tu, X.-h. Xia, X.-l. Wang, C.-d. Gu, Hydrothermally synthesized WO_3 nanowire arrays with highly improved electrochromic performance, J. Mater. Chem. 21 (2011) 5492–5498.
[21] J. Wang, P.S. Lee, J. Ma, Cryst. Growth Des. 9 (2009) 2293–2299.
[22] L. Zhou, J. Zou, M. Yu, P. Lu, J. Wei, Y. Qian, Y. Wang, C. Yu, Green synthesis of hexagonal-shaped $WO_3{\cdot}0.33H_2O$ nanodiscs composed of nanosheets, Cryst. Growth Des. 8 (2008) 3993–3998.
[23] X. Chang, S. Sun, Y. Yin, Green synthesis of tungsten trioxide monohydrate nanosheets as gas sensor, Mater. Chem. Phys. 126 (2011) 717–721.
[24] W. Li, E. Shi, W. Zhong, Z. Yin, Growth mechanism and growth habit of oxide crystals, J. Cryst. Growth. 203 (1999) 186–196.
[25] Z. Chen, E. Shi, Y. Zheng, W. Li, B. Xiao, J. Zhuang, Growth of hex-pod-like Cu_2O whisker under hydrothermal conditions, J. Cryst. Growth. 249 (2003) 294–300.
[26] J. Zhang, J. Tu, X. Xia, X. Wang, C. Gu, Hydrothermally synthesized WO_3 nanowire arrays with highly improved electrochromic performance, J. Mater. Chem. 21 (2011) 5492–5498.
[27] N. Wu, E. Shi, Y. Zheng, W. Li, Effect of pH of medium on hydrothermal synthesis of nanocrystalline cerium(IV) oxide powders, J. Am. Ceram. Soc. 85 (2002) 2462–2468.